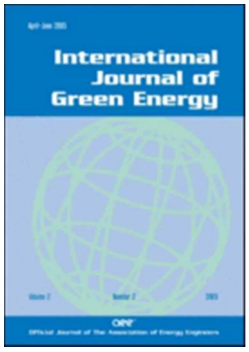

Energy Generation from full strength Domestic Wastewater using a Sandwich Dual Chamber Microbial Fuel Cell with an uncatalyzed Mesh Current Collector Cathode

Journal:	*International Journal of Green Energy*
Manuscript ID:	IJGE-2015-0274
Manuscript Type:	Regular Paper
Date Submitted by the Author:	02-Jun-2015
Complete List of Authors:	ADENIRAN, JOSHUA; UNIVERSITY OF JOHANNESBURG, CIVIL ENGINEERING TECHNOLOGY Huberts, Robert; UNIVERSITY OF JOHANNESBURG, CHEMICAL ENGINEERING TECHNOLOGY de Koker, Johan; UNIVERSITY OF JOHANNESBURG, SUSTAINABLE ENERGY TECHNOLOGY AND RESEARCH CENTRE, SeTAR AROTIBA, OMOTAYO; UNIVERSITY OF JOHANNESBURG, APPLIED CHEMISTRY VAN ZYL, ERICK; UNIVERSITY OF JOHANNESBURG, BIOTECHNOLOGY DU PLESSIS, SYDNEY; UNIVERSITY OF JOHANNESBURG,
Keywords:	Microbial Fuel Cells, power generation, domestic wastewater, mesh current collector , cathode

SCHOLARONE™
Manuscripts

Energy Generation from full strength Domestic Wastewater using a Sandwich Dual Chamber Microbial Fuel Cell with an uncatalyzed Mesh Current Collector Cathode

JA Adeniran[1], R Huberts[2]*, JJ De-Koker[3], OA Arotiba[4], E Van-Zyl[5] and S Du-Plessis[6]

[1]Department of Civil Engineering Technology, [2]Department of Chemical Engineering Technology, [3] Sustainable Energy Technology and Research Centre, SeTAR ,[4]Department of Applied Chemistry ,[5]Department of Biotechnology and [6]Metallurgy Department, University of Johannesburg, P.O. Box 17011, Doornfontein 2028, Johannesburg, South Africa.

**Corresponding author: roberth@uj.ac.za*

For Peer Review Only

Abstract

A sandwich domestic wastewater fed dual-chamber microbial fuel cell (MFC) was designed for energy generation and wastewater treatment. Power density for the MFC increased with increasing domestic wastewater concentration, reaching a maximum of 251 mW/m^2 for full strength wastewater (3400 mg/L chemical oxygen demand (COD)) at a current density of 0.054 mA/cm^2 at an external resistance of 200Ω. These values dropped to 60 mW/m^2 (76% lower) and 0.003 mA/cm^2 using wastewater 91% diluted to 300 mg/L COD. Maximum removals were: of COD, 89%; nitrite, 60%; nitrate, 77%; total nitrogen, 36%; and phosphate, 26%. Coulombic efficiency ranged from 5% to 7%. The use of full strength domestic wastewater reduces cost, and with improved reactor design, the ultimate goal of large scale operation could be achieved.

Key words: Microbial Fuel Cells, power generation, domestic wastewater, mesh current collector cathode

1. Introduction

In the early days of microbial fuel cell (MFC) research, most of the studies were carried out using the conventional dual-chamber MFC. However, the recent trend in MFC research involves the use of single-chamber MFCs. This is in accordance with reports of higher power and current densities generated from single-chamber MFCs compared with dual-chamber MFCs. Higher internal resistance and electron acceptor limitations are among the major factors that restrict power generation in dual-chamber MFCs. In MFC studies, in a bid to increase power generation, the impact of various materials used in the construction of reactors has been investigated. The use of catalyzed cathodes built around mesh current collectors used in single-chamber MFCs has been reported to increase power generation significantly (Luo et al. 2011; Zhang et al. 2009, 2010, 2011). Mesh pore sizes also play an important role in increasing power density in MFCs. In a study by Zhang and coworkers (2011), the effect of cathode mesh pore size on power generation was ascertained, using five stainless steel meshes of different pore sizes (30, 50, 70, 90 and 120), treated with poly(dimethylsiloxane) (PDMS) and Pt, as cathode in a single-chamber cubic-shaped MFC. The results indicated direct proportionality between pores sizes and power density. Mesh 30 recorded the highest maximum power density of 1616 ± 25 mW/m^2, while the lowest power density of 599 ± 57 mW/m^2 was obtained with mesh 120 which has the smallest pore size. A further investigation into the use of these mesh pore sizes may be helpful in increasing the power generation and efficiency of MFCs.

Despite the aforementioned advantages of single-chamber MFCs over dual-chamber MFCs, the shortcomings of lower coulombic efficiency (in comparison with dual chambers) (Zhang et al. 2009; Liu et al. 2004) and leakage of the anode solution through the cathode (Zhang et al. 2009) reported in single-chamber MFCs need to be overcome to maximize the potential of MFC technology for energy generation and wastewater treatment. An improvement in the design of dual-chamber MFCs in terms of architecture

For Peer Review Only

and materials of construction may be a viable alternative way of overcoming the limitations of single-chamber MFCs. In this study, a dual-chamber MFC with reduced electrode spacing was developed and tested for energy generation from domestic wastewater. In addition, the impact of wastewater organic materials concentration (wastewater concentration) in the anode chamber on energy generation was ascertained.

Mesh current collectors have been used previously as cathode electrodes in single-chamber MFC studies (Xia et al. 2013; Luo et al. 2011; Zhang et al. 2009, 2010, 2011). However, to the best of our knowledge, this is the first study involving a combined use of mesh current collector cathode electrode and sandwich electrodes architectures in a dual-chamber MFC.

2. Materials and Methods

2.1. Cathode

The cathode was constructed from stainless steel mesh 20 type 304 (0.37 mm diameter, 0.90 mm opening, 737 MPa tensile strength and 39% elongation). The stainless steel mesh was supplied by Ludowisi Meshcape, South Africa (SA). The cathode electrode was uncatalyzed, with a projected surface area of 36 cm^2, a thickness of 0.72 mm and a total weight of 6.60 g. Details of the mesh material used are provided in Table 1.

(Table 1)

2.2. MFC construction and operation

2.2.1. Sandwich Electrode Membrane Electrode Configuration, SEMEC

A sandwich consisting of the anode (non-wet proof carbon fabric, 1071HCB, Avcarb, NJ), the proton exchange membrane (CMI 7000S, Membranes International Inc., NJ) and the cathode electrode was glued to the anode chamber (polyethylene wide-mouth bottle). This is illustrated schematically in Figure 1. The anode compartment had a total volume of 2000 mL and was filled with 1500 mL of domestic wastewater

URL: http://mc.manuscriptcentral.com/green-energy Email: x6li@mecheng1.uwaterloo.ca

For Peer Review Only

(1500 mL empty bed volume). The anode electrode had a surface area of 36 cm^2, and the sandwich weighed 10.6 g. Thereafter, the entire structure was placed in a temperature-regulated water bath (Ecobath, Labotech, South Africa) containing the cathode solution. The water bath's in-built circulator replenished the dissolved oxygen used as the electron acceptor at the cathode.

(Figure 1)

2.2.2. MFC Operation

The reactor was inoculated with primary sludge and domestic wastewater from Daspoort wastewater treatment works, Pretoria, South Africa and subsequently fed with domestic wastewater after a repeatable current production had been established. The reactor was a semi-continuous one operated on a long fed batch cycle (fed with 500 mL fresh influent once a week), at 35 °C. Hence a wastewater residence time of 3 weeks was achieved. The cathode solution was maintained at pH of approximately 1.88, while the anode solution was operated at an average pH of 7.5. The CODs of the influent and effluent were determined using HACH COD system (HACH Co., Loveland, CO., USA).

2.3 MFC calculations and measurements

The voltage (V) across the external resistor was measured at 5-minute intervals after a pseudo-steady state had been established. The power ($P = IE_{MFC}$) and current ($I = \frac{E_{MFC}}{R_{ext}}$) produced by the reactor were determined by measuring the potential across the external resistor, as described by Logan (2008) and Logan et al. (2006). E_{MFC} and R_{ext} represent the cell potential (volts) and external resistance or load (ohm) respectively. Polarization and power density curves were obtained by varying the external circuit resistance from 2 400 Ω to 50 Ω in decreasing order. Power and current densities were normalized to the projected surface area of the cathode (36 cm^2) at R_{ext} 200 Ω, except when stated otherwise.

The MFC internal resistance was calculated using the polarization slope method. This was achieved by calculating the slope of the polarization curve, using the formula given by Logan (2008):

For Peer Review Only

$$R_{\text{int}} = \frac{\Delta \text{E}}{\Delta \text{I}} \quad (1)$$

where ΔE is the change in voltage and ΔI is the change in current. The columbic efficiency (CE) was determined from the COD removed per cycle of operation (Logan et al. 2006) using the following formula also given by Logan (2008):

$$CE = \frac{\text{M}_S \text{I} t_b}{F b_{es} V_{an} \Delta_{COD}} \quad (2)$$

where M_S is the molecular weight of substrate (g/mol), I is the current density (mA/cm^2), t_b is the operation time (h), Fb_{es} is the Faraday's constant [(96500 C/ mole$^-$) (8 mole$^-$/ mol)], V_{an} is the volume of the anode (L) and Δ_{COD} is the change in COD (g/L).

Electrochemical characterization (open circuit potential (OCP) and cyclic voltammetry) of the mesh electrode was conducted on an Ivium CompactStat potentiostat (Netherlands). A three-electrode system consisting of a stainless steel mesh (cathode in the MFC) as working electrode, a platinum counter electrode and an Ag/AgCl reference electrode (RE-5B; BASi; West Lafayette, IN) was employed. The tests were conducted using three different solutions. The first solution was a mixture of 50% cathode solution (water and sulphuric acid) and 50% 10 mM phosphate buffer solution (PBS) (made up of Na_2HPO_4 0.458 g/L + $Na_2HPO_4.H_2O$ 0.245 g/L). The second solution consisted of 50% 50 mM PBS and 50% cathode solution, while the third solution was the cathode solution without a supporting electrolyte. The cyclic voltammetry scan rate was + 0.50 mV/s and the potential was scanned from + 1.0 to - 0.4 V.

For Peer Review Only

2.4. Nutrient removal analysis

In order to determine the efficiency of the reactor for wastewater treatment, concentrations of nitrate, nitrite, total nitrogen and phosphate were analyzed in the influents and effluents using Hach techniques (HACH Co., Loveland, CO, USA.). Prior to the analysis, the samples were centrifuged to ensure homogeneity. All analyses were carried out in triplicate and the average reported to ensure reproducibility of the results. For nitrate (cadmium reduction method, 0.3–30.0 mg/L $NO_3^- N$); nitrite (ferrous sulphate method, nitriVer2 , 2–250 mg/L NO_2^- reagent powder pillows); total nitrogen (persulphate digestion method, 2–150 mg/L N, test tube and vials) and phosphate (molybdovanadate method 0.3–45.0 mg/L PO_4^{3-}, reagent solution), the methods indicated in the respective brackets were used for the analyses.

The nutrient removals were determined using the formula:

$$C_{removed} = \frac{C_{\inf luent} - C_{effluent}}{C_{\inf luent}} \times 100\ \% \quad (3)$$

where $C_{removed}$ *is* the nutrient removed (%), $C_{\inf luent}$ is the influent nutrient concentration (mg/L) and $C_{effluent}$ is the effluent nutrient concentration (mg/L).

2.5. Wastewater Organic matter concentration measurement

The influent and effluent organic matter concentrations were determined by carrying out COD analysis, hence wastewater COD concentration was used as a measure of organic matter concentration in this study. The analyses were done in triplicate and the average reported, using the Hach COD system (Hach,

For Peer Review Only

Loveland, CO, USA). The wastewater strength was varied from 3400 to 300 mg/L by dilution with deionized water to ascertain the effect of substrate organic matter concentration on power generation. The COD removal (%) was calculated using the formula:

$$X_r = \frac{X_i - X_e}{X_i} \times 100\% \quad (4)$$

where X_r is the COD removed (%), X_i is the influent COD (mg/L) and X_e is the effluent COD (mg/L).

2.6. Electron microscopy examination

Scanning electron microscope (SEM) images of the anode were taken to observe biofilm growth using a VEGA3 TESCAN (TESCAN Brno-Kohoutovice, Czech Republic). The anode electrodes (working and control) were cut into small pieces (about 1 cm x 1 cm) and fixed overnight in 2.5% paraformaldehyde and 1.5% glutaraldehyde in 0.1 M cacodylate buffer, pH 7.4 at 4 °C. They were washed three times in the buffer, dehydrated in graded ethanol solutions and dried at the critical point using carbon dioxide (Liu & Logan 2004). Thereafter the samples were gold sputter-coated using an Emscope SC 500 gold coater.

3. Results and Discussion

3.1. Organic matter concentration and power generation

The effect of wastewater COD concentration on power production was examined by comparing the power density at the highest substrate COD concentration (PDH) and the polarization (PCH) curves with those at the lowest COD concentration (PDL and PCL) (Figure 2(a)). The maximum power generation from the MFC at various COD concentrations is represented in Figure 2(b).

Maximum power density of 251 mW/m^2 and current density of 0.059 mA/cm^2 were generated at the highest COD (3400 mg/L). In turn, the lowest power density (60 mW/m^2) and current density (0.03 mA/cm^2) were generated when wastewater of the lowest COD concentration of 300 mg/L was fed (Figure

For Peer Review Only

2(a)), representing a 76% drop in power density. Throughout the course of the experiments, a general trend of reduction in power production with COD reduction was observed (Figure 2(b)). This is similar to findings in previous studies (Zhong et al. 2011; Rodrigo et al. 2007) where high substrate concentration increased power density in MFCs. This finding is also consistent with findings in some previous studies that power generation in MFCs depends on wastewater concentration (Liu et al. 2005; Min et al. 2005). In the same vein, the observation is similar to reports of increased power generation with feed concentration (Moon et al. 2006), where highest power and current densities of 0.36 W/m^2 and 1.6 A/m^2 respectively were reported at the highest fuel concentration of 300 mg/L. The results, however, differ from the findings by Zhong et al. (2011) where COD concentration was found not to be the only limiting factor in power generation. In their study, Zhong and coworkers investigated power generation at three organic loading rates (OLRs), viz. 6.00, 3.20 and 1.55 kg COD $m^{-3}d^{-1}$. The lowest power density of 74.0 ± 1.8 mW/m^2 (0.65 ± 0.02 mW^{-3}) was recorded at 6.00 kg COD $m^{-3}d^{-1}$, followed by 92.1 ± 3.3 mW/m^2 (0.081 ± 0.03 mW^{-3}) at 1.55 kg COD $m^{-3}d^{-1}$, and with a maximum power density of 115.5 ± 2.7 mW/m^2 (1.0 ± 0.02 mW^{-3}) being generated at 3.20 kg COD $m^{-3}d^{-1}$. It was reported that factors such as poisoning of the catalyst (Pt) at high organic matter concentration and fouling of the catalyst layer by biofilm could be partly responsible for the development. However, in this study no catalyst was applied to the electrodes, which could be responsible for the different observations. The maximum average power density of 251 mW/m^2 obtained in this study is higher than the power densities reported in previous natural wastewater-fed dual-chamber MFC studies: 63 mW/m^2 (Min & Logan 2004) using domestic wastewater in a flat plate MFC; 45 mW/m^2 (Min et al. 2005) when swine wastewater was used as substrate; and 25 mW/m^2 (Rodrigo et al. 2007) using urban wastewater.

(Figure 2a)

(Figure 2b)

For Peer Review Only

It can be seen from Table 2 that the maximum power density reported in this work compares favourably with that of most studies in which natural wastewaters were used as substrates in MFCs. This suggests that the sandwich dual-chamber MFC designed for this work is efficient in terms of power generation, taking into consideration the fact that dual-chamber MFCs are known to generate lower power densities than single-chamber MFCs (Logan 2008).

(Table 2)

3.2. Internal resistance

The internal resistance (R_{int}) of the reactor was determined using the polarization slope method (Logan, 2008). The internal resistances recorded were inversely proportional to the COD concentration (Figure 3), with the highest R_{int} of 376 Ω recorded at 300 mg/L COD concentration and the minimum R_{int} of 80 Ω at a COD concentration of 3400 mg /L. This is consistent with the results of Feng et al. (2008) who found that R_{int} decreased with an increase in COD concentration. The minimum R_{int} of 80 Ω is high compared with some of the previously reported results (Fan et al. 2007; Cheng et al. 2006), but lower than the 1632 Ω reported by You et al. (2006) when permanganate was used as the electron acceptor in a dual-chamber MFC. A maximum R_{int} of 376 Ω was recorded in this study (Figure 3). This is higher than (159 ± 11 Ω, 184 ± 15 Ω and 216 ± 8 Ω) using lactic acid, acetic acid and ethanol respectively as substrates and equal to 376 ± 30 Ω (succinic acid substrate) reported in the study by Kiely and fellow workers (2011). However, it is significantly lower than 2769 ± 318 Ω obtained in the same study (Kiely et al. 2011) when formic acid was used as a substrate. Bearing in mind that solution conductivity affects power generation in MFCs due to its impact on ionic flow (Logan 2012), and the fact that domestic wastewater is known for low conductivity, full-strength domestic wastewater (698 ± 81 µs/cm) was used as substrate in this study. The low substrate conductivity is believed to be responsible for the relatively high internal resistance (R_{int}).

For Peer Review Only

(Figure 3)

From the polarization curve in Figure 4 it can be deduced that activation losses were prominent from 0 to 0.033 mA/cm^2, as depicted by the first high gradient (I) in region A. The ohmic region between 0.033 mA/cm^2 and 0.072 mA/cm^2, denoted by region B, can be observed to be characterized by the relatively steady rise in gradient, and the mass transport losses can be observed from 0.072 to 0.127 mA/cm^2, characterized by a steep rise in gradient (region C). The magnitude of the activation loss observed in this figure could be attributed to the use of an uncatalyzed electrode and the relatively high energy required for the oxidation and reduction reaction due to the high COD concentration of the wastewater (Logan 2008). Ohmic losses represent one of the major challenges to be overcome in the design of a scalable MFC (Logan 2008). Although a sandwich MFC design known for reduced internal resistance (Liu et al. 2004) was used for the experiments, the use of a membrane (PEM) in this study could be responsible for the relatively large interval of ohmic losses observed in the polarization curve in Figure 4 (Logan et al. 2006). The observation of mass transport losses in the polarization curve is an indication of the need to improve the reactant and product flux on the electrodes (Logan 2008).

(Figure 4)

3.3. Nutrient removal and coulombic efficiency

Table 3 presents the wastewater treatment efficiency using the percentage of nutrients removed as an indicator. We attribute the removal of nitrate and phosphate to a process caused by the bacteria consortium in our wastewater. The nitrate removal is also an indication of a de-nitrification process in our reactor.

The reason for the relatively lower total nitrogen removal (36%), compared with nitrate (77%) and nitrite (66%), is not well understood at this stage. However, since total nitrogen contains both organically bound nitrogen and oxidizable nitrogen (nitrite and nitrate) we assumed that endogenous decay of the

For Peer Review C

microorganisms in the wastewater might have resulted in the release of organically bound nitrogen, as noted by Bahadoorsingh (2010). This happens during a long retention time and with a low ratio of substrate to microorganisms, leading to autolysis which causes a release of large quantities of organic matter (Miura et al. 2007). We hypothesize that the relatively long residence time of the wastewater in the MFC (3 weeks) could favour endogenous decay. This phenomenon will lead to the release of the organically bound nitrogen component of the total nitrogen, hence its relatively higher concentration in the effluent compared with nitrite and nitrate.

A better measure of the extent of wastewater treatment in the MFC is COD measurement. A maximum COD removal of 89% was recorded in this study, signifying an efficient wastewater treatment. The high COD removal (89%) and low CE values (5–7%) also support the assumption of nutrient removal by bacteria, possibly other than the exoelectrogenic bacteria. A similar finding was made by He at al. (2005), who recorded a soluble chemical oxygen demand (SCOD) removal of 90% and CEs of 0.7–8.1% in an upflow MFC. The findings were attributed to oxidation of the anodic substrates by bacteria other than the exoelectrogens.

(Table 3)

From Figure 5 it can be seen that the CE during the course of the experiment ranged from 5 to 7%. The maximum CE was recorded between wastewater concentrations of 300 and 800 mg/L, with the lowest CE recorded between 2200 and 3400 mg/L. The relationship between CE and substrate concentration is inverse, which is similar to the observations by Min and coworkers (2005). The CE obtained in this study is poor (maximum of 7%) and this suggests that the reactor was not efficient in converting the organic matter in wastewater to energy. It is also an indication that the design needs to be further optimized for improved energy generation. The relatively longer cycle of operation (7 days) could be partly responsible for the low CE recorded because of the potential increase in oxygen influx to the anode due to the increase in operation time. This is consistent with the findings of Feng et al. (2008). Further efforts need

For Peer Review Only

to be made to prevent the influx of oxygen into the anodic chamber to prevent scavenging of electrons by oxygen.

(Figure 5)

From Figure 6 it is evident that COD removal is proportional to wastewater concentration. The maximum COD removal of 89% was recorded at the highest COD concentration (3400 mg/L). This observation is consistent with the findings by Wang et al. (2008), where COD removal increased with wastewater concentration, resulting in a maximum COD removal of 87% at the highest wastewater COD concentration of 2339 mg/L. Also, considering the volume of wastewater in the anode chamber (1.5 L) and the fact that full-strength wastewater was employed (at the maximum COD concentration reported, 3400 mg/L), this result shows the potential of the MFC as a wastewater treatment technique.

(Figure 6)

3.4. Electrochemical analysis

The cathode OCP was 0.343 mV vs. Ag/AgCl. This result was higher than the cathode OCP of 0.230 V vs. Ag/AgCl reported by Liu and Logan (2004) when the MFC was operated without a PEM. An average OCV of 0.735 ± 0.1 V was recorded, a result that is fairly close to the maximum OCV of 0.8V reported in single-chamber MFCs using oxygen as electron acceptor (Cheng & Logan, 2007).

The appearance of capacitive currents and faradaic peaks in the CV (Figure 7) suggests that the electrode (stainless steel mesh cathode) is conducting and is suitable for MFC application.

(Figure 7)

3.5. Scanning Electron Micrograph analysis of anode electrode

For Peer Review Only

The scanning electron micrograph results of the surface morphology of the anode electrode are depicted in Figure 8. The result reveals the growth of biofilm on the working electrode (Figure 4.8A i, ii and iii) at different magnifications compared with none on the control electrode (Figure 4.8B i, ii and ii). This indicates the colonization of the electrode by the bacteria consortia in the wastewater (Park et al., 2005). The exoelectrogenic bacteria in the wastewater are believed to be responsible for the anodic oxidation reaction leading to electricity generation (Muthukumar & Sangeetha, 2014).

(Figure 8)

4.0. Conclusions

A relatively low-cost sandwich dual-chamber microbial fuel cell (MFC) was constructed for energy generation and domestic wastewater treatment. The successful incorporation of the sandwich electrode membrane electrode configuration and an uncatalyzed mesh current collector cathode into the dual-chamber MFC increased power production, wastewater treatment efficiency and at the same time reduced the cost. Furthermore, the use of a relatively larger reactor (1.5 L empty bed volume), compared with most of the MFCs reported in the literature, lends credence to the upscaling potential of this reactor for full-scale energy generation and wastewater treatment.

5.0. Acknowledgements

We thank the University of Johannesburg for supporting this project. This research was co funded with National Research Fund (NRF) THRIP Grant UID: 90260 and ESKOM Grant (Energy generation from Microbial Fuel Cell). Also, we appreciate the Young Water Professional (YWP), South Africa for facilitating a research writing workshop at the University of Johannesburg in January 2014 where the first author was further exposed to the art of writing scientific articles.

URL: http://mc.manuscriptcentral.com/green-energy Email: x6li@mecheng1.uwaterloo.ca

For Peer Review Only

For Peer Review Only

6.0. References

Bahadoorsingh, P., 2010. Comparison of nitrification activity in membrane and conventional enhanced biological phosphorus removal processes. PhD Thesis, *University of British Columbia*, Vancouver, Canada.

Cheng, S., H. Liu, and B.E. Logan. (2006). Increased power generation in a continuous flow MFC with advective flow through the porous anode and reduced electrode spacing. *Environmental Science and Technology* 40: 2426─2432.

Cheng, S., and B.E. Logan. (2007). Ammonia treatment of carbon cloth anodes to enhance power generation of microbial fuel cells. *Electrochemistry Communications* 9: 492─496.

Fan, Y., H. Hu, and H. Liu. (2007). Sustainable power generation in microbial fuel cells using bicarbonate buffer and proton transfer mechanisms. *Environmental science and technology* 41: 8154─8158.

Feng, Y., X. Wang, B.E. Logan, and H. Lee. (2008). Brewery wastewater treatment using air-cathode microbial fuel cells. *Applied Microbiology and Biotechnology* 78: 873─880.

He, Z., S.D. Minteer, and L.T. Angenent. (2005). Electricity generation from artificial wastewater using an upflow microbial fuel cell. *Environmental Science and Technology* 39: 5262─5267.

Kiely, P.D., G. Rader, J.M. Regan, and B.E. Logan. (2011). Long-term cathode performance and the microbial communities that develop in microbial fuel cells fed different fermentation end products. *Bioresource Technology* 102: 361─366.

Logan, B E., B. Hamelers, R. Rozendal, U. Schrorder, J. Keller, S. Freguia, P. Aelterman, W. Verstraete, and K. Rabaey. (2006). Microbial fuel cells: Methodology and technology. *Environmental Science and Technology* 40:5181─5192.

Liu, H., and B.E. Logan. (2004). Electricity generation using an air-cathode single chamber microbial fuel cell in the presence and absence of a proton exchange membrane. *Environmental Science and Technology* 38:4040─4046.

Liu, H., S. Cheng, and B.E. Logan. (2005). Production of electricity from acetate or butyrate using a single-chamber microbial fuel cell. *Environmental Science and Technology* 39:658─662.

Logan, B.E., B. Hamelers, R. Rozendal, U. Schröder, J. Keller, S. Freguia, P. Aelterman, W. Verstraete, and K. Rabaey. (2006). Microbial fuel cells: methodology and technology. *Environmental Science and Technology* 40: 5181─5192.

Logan, B.E. (2008). Microbial Fuel Cells. New Jersey: *John Wiley and Sons, Inc*.

Logan, B.E. (2012). Essential data and techniques for conducting microbial fuel cell and other types of bioelectrochemical system experiments. *ChemSusChem* 5: 988─994.

Luo, Y., F. Zhang, B. Wei, G. Liu, R. Zhang, and B.E. Logan. (2011). Power generation using carbon mesh cathodes with different diffusion layers in microbial fuel cells. *Journal of Power Sources* 196:9317─9321.

For Peer Review Only

Min, B., and B. Logan.2004. Continuous electricity generation from domestic wastewater and organic substrates in flat plate microbial fuel cell. *Environmental Science and Technology* 38:5809─5814.

Min, B., J.R. Kim, S.E. Oh, J.M. Regan, and B.E. Logan. (2005). Electricity generation from swine wastewater using microbial fuel cell. *Water Research* 39:4961─4968.

Miura, Y., M.N. Hiraiwa, T. Ito, T. Itonaga, Y. Watanabe, and S. Okabe. (2007). Bacterial community structures in MBRs treating municipal wastewater: relationship between community stability and reactor performance. *Water Research* 41: 627─637.

Moon, H., I.S. Chang, and B.H. Kim. (2006). Continuous electricity production from artificial wastewater using a mediator-less microbial fuel cell. *Bioresource Technology* 97: 621─627.

Muthukumar, M., and T. Sangeetha. (2014). The Harnessing Of Bioenergy From A Dual Chambered Microbial Fuel Cell (MFC) Employing Sago-Processing Wastewater As Catholyte. *International Journal of Green Energy* 11:161─172.

Park, H.I., Y., Choi, and D. Pak, D. (2005). Nitrate reduction using an electrode as direct electron donor in a biofilm-electrode reactor. *Process Biochemistry* 40:3383─3388.

Rodrigo, M., P. Cañizares, J. Lobato, R. Paz, C. Sáez, and J. Linares. (2007). Production of electricity from the treatment of urban wastewater using a microbial fuel cell l. *Journal of Power Sources* 169:198─204.

Wang, X., Feng, Y. and H. Lee. (2008). Electricity production from beer brewery wastewater using single chamber microbial fuel cell. *Water Science and Technology* 57: 1117─1122.

Wang, X.,Y. Feng, H. Wang, Y. Qu, Y. Yu, N. Ren, N. Li, E. Wang, H. Lee, and B.E. Logan. (2009). Bioaugmentation for electricity generation from corn stover biomass using microbial fuel cells. *Environmental Science and Technology* 43: 6088─6093.

For Peer Review Only

Wen, Q., Y. Wu, D. Cao, L. Zhao, and Q. Sun. (2009). Electricity generation and modeling of microbial fuel cell from continuous beer brewery wastewater. *Bioresource Technology* 100:4171─4175.

Xia, X., F. Zhang, X. Zhang, P. Liang, X. Huang, and B.E. Logan. (2013). Use of Pyrolyzed Iron Ethylenediaminetetraacetic Acid Modified Activated Carbon as Air–Cathode Catalyst in Microbial Fuel Cells. *ACS Applied Materials and Interfaces* 5:7862─7866.

You, S., Q. Zhao, J. Zhang, J. Jiang, and S. Zhao. (2006). A microbial fuel cell using permanganate as the cathodic electron acceptor. *Journal of Power Sources* 162:1409─1415.

Zhang, F., S. Cheng, D. Pant, G. Van Bogart, and B.E. Logan. (2009). Power generation using an activated carbon and metal cathode in a microbial fuel cell. *Electrochemistry Communications* 11: 2177─2179.

Zhang, F., T. Saito, S. Cheng, M.A. Hickner, and B.E. Logan. (2010). Microbial fuel cell cathodes with poly (dimethylsiloxane) diffusion layers constructed around stainless steel mesh current collectors. *Environmental Science and Technology* 44:1490─1495.

Zhang, F., M.D. Merrill, J.C. Tokash, T. Saito, S. Cheng, M.A. Hickner, and B.E. Logan. (2011). Mesh optimization for microbial fuel cell cathodes constructed around stainless steel mesh current collectors. *Journal of Power Sources* 196: 1097─1102.

Zhong, C, B. Zhang, L. Kong, A. Xue, and J. Ni. (2011). Electricity generation from molasses wastewater by an anaerobic baffled stacking microbial fuel cell. *Journal of Chemical Technology and Biotechnology* 86: 406─413.

For Peer Review Only

Figure 1 Schematic representation of MFC design

Figure 2a Polarization and power curves at lowest and at highest COD

Figure 2b Power density as a function of COD concentration

Figure 3 Internal resistance relationship with substrate concentration

Figure 4 Polarization curve of the MFC at the highest COD (3400 mg/L)

Figure 5 Effects of wastewater COD concentration on CE and COD removal

Figure 6 Wastewater concentration effect on COD removal

Figure 7 CV of SS mesh cathode in cathode solution

Figure 8 Scanning electron micrograph of anode (working electrode) inoculated with domestic wastewater (A) and (B) a control electrode (before inoculation)

Table 1 Mesh material and chemical composition

Table 2 Selected maximum power densities using natural wastewater in MFCs

Table 3 Summary of the wastewater treatment efficiency analysis of the MFC

For Peer Review Only

Energy Generation from full strength Domestic Wastewater using a Sandwich Dual Chamber Microbial Fuel Cell with an uncatalyzed Mesh Current Collector Cathode

For Peer Review Only

Figure 1 Schematic representation of MFC design

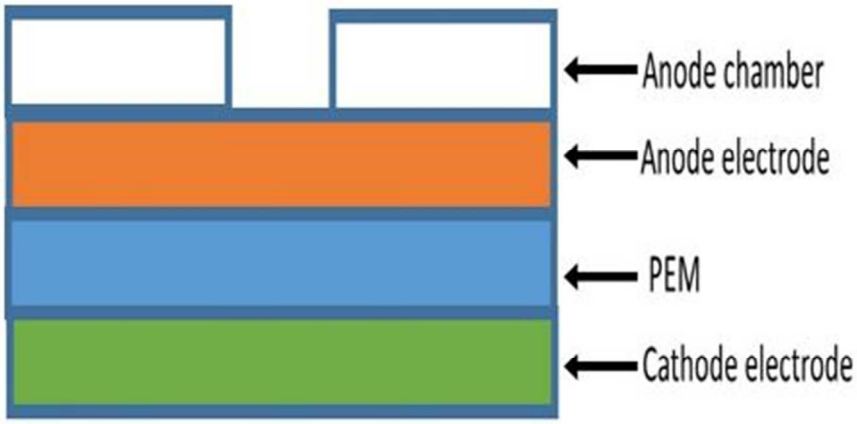

Schematic representation of MFC design
135x98mm (96 x 96 DPI)

View Only

Figure 2(a) Polarization and power curves at lowest and at highest COD

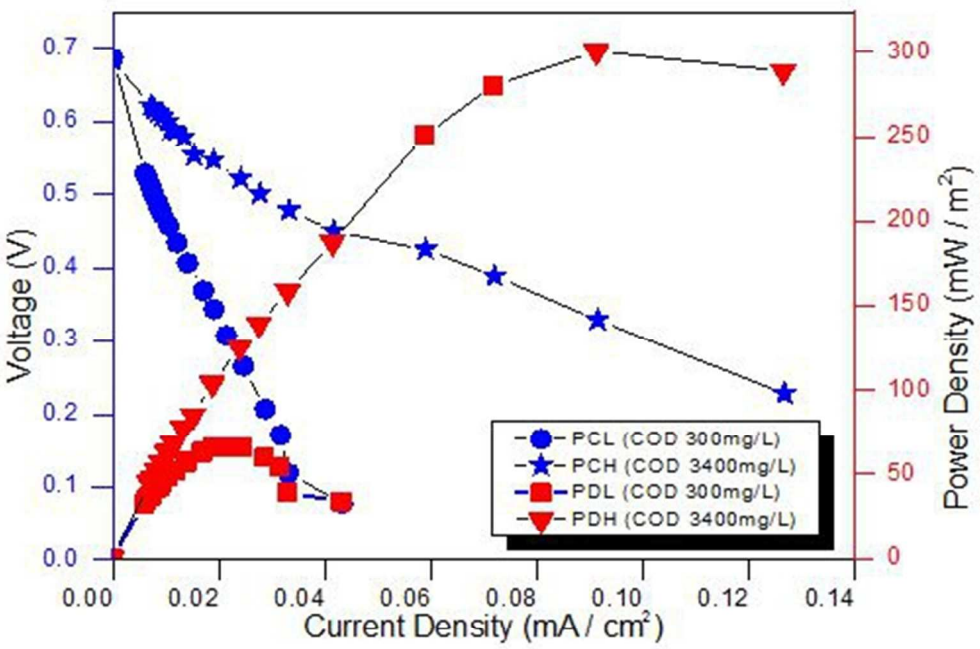

Polarization and power curves at lowest and at highest COD
135x117mm (96 x 96 DPI)

For Review Only

Figure 2(b) Power density as a function of COD concentration

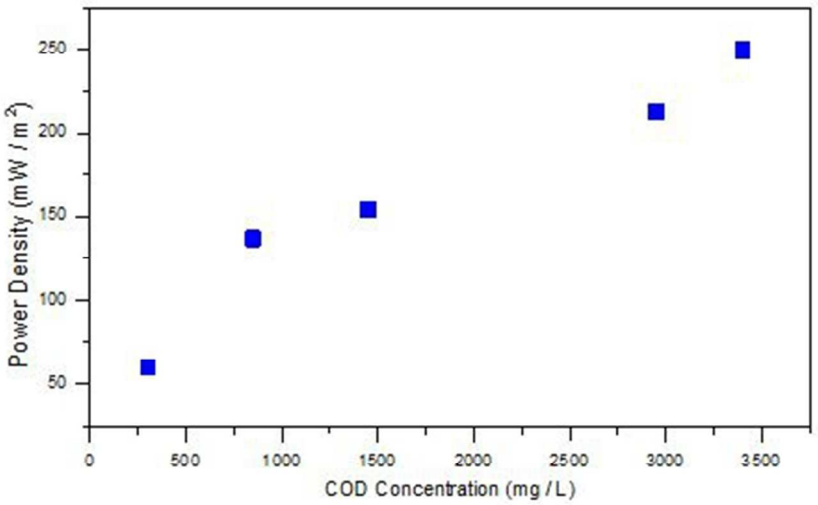

Power density as a function of COD concentration
142x102mm (96 x 96 DPI)

View Only

Figure 3 Internal resistance relationship with substrate concentration

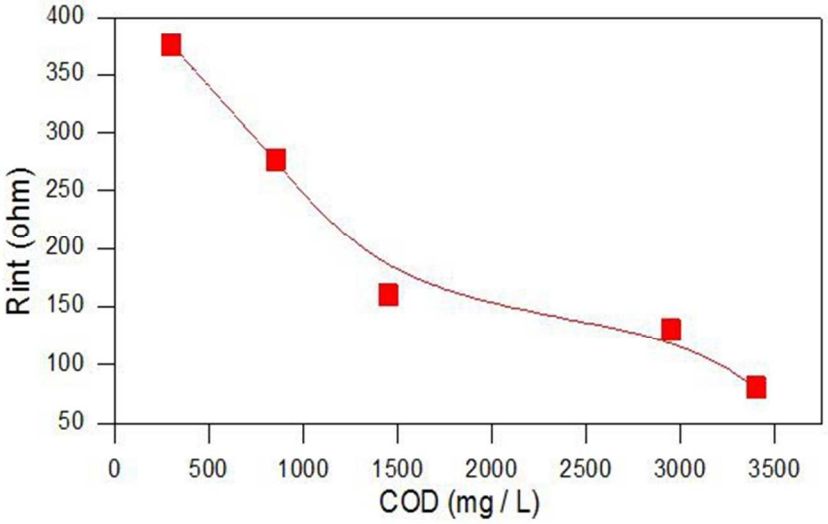

Internal resistance relationship with substrate concentration
174x124mm (96 x 96 DPI)

view Only

Figure 4 Polarization curve of the MFC at the highest COD (3400 mg/L)

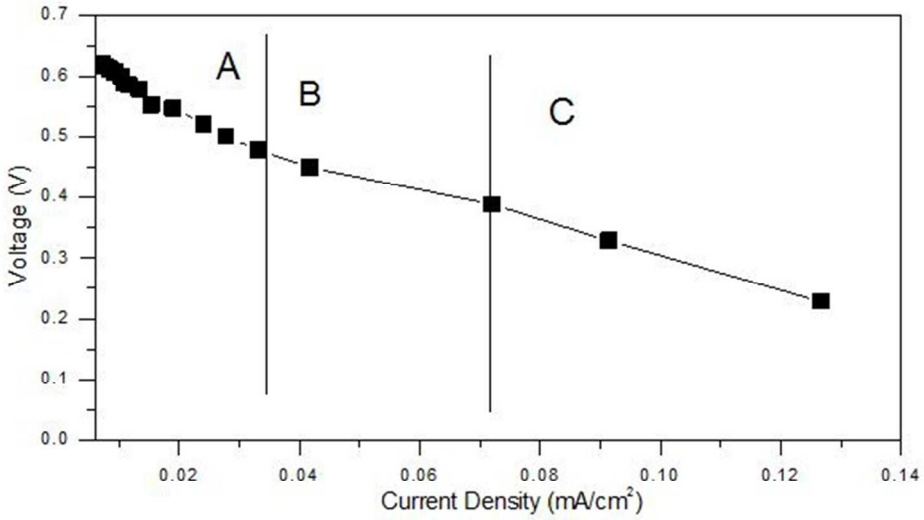

Polarization curve of the MFC at the highest COD (3400 mg/L)
165x115mm (96 x 96 DPI)

For Review Only

Figure5 Effects of wastewater COD concentration on CE and COD removal

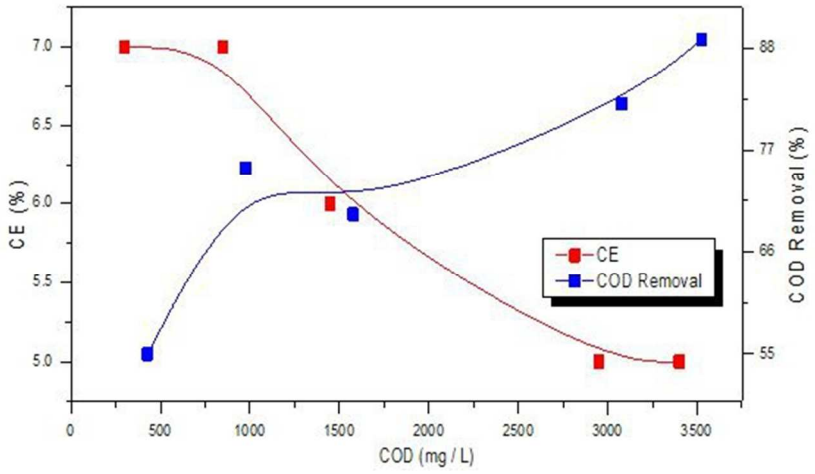

Effects of wastewater COD concentration on CE and COD removal
180x124mm (96 x 96 DPI)

For Review Only

Figure 6 Wastewater concentration effect on COD removal

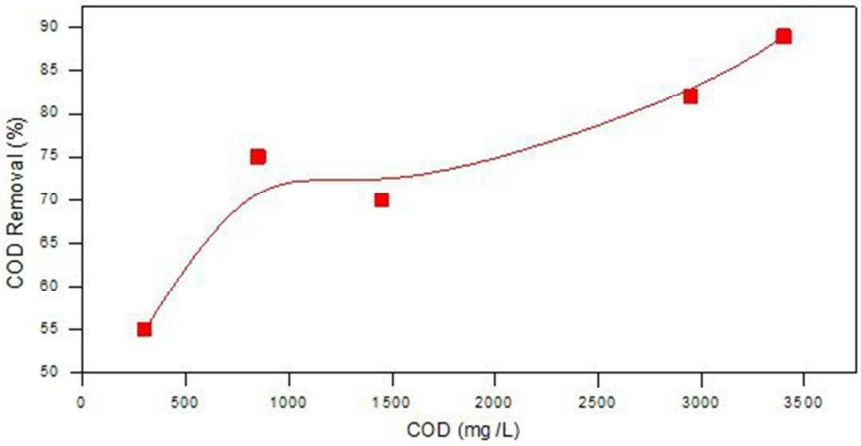

Wastewater concentration effect on COD removal
166x113mm (96 x 96 DPI)

For Review Only

Figure 7 CV of SS mesh cathode in cathode solution

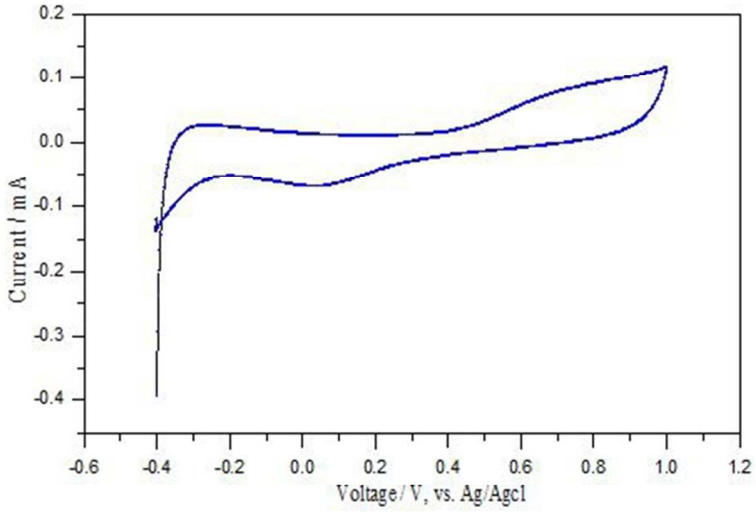

CV of SS mesh cathode in cathode solution
158x113mm (96 x 96 DPI)

View Only

Figure 8 Scanning electron micrograph of anode (working electrode) inoculated with domestic wastewater (A) and (B) a control electrode (before inoculation)

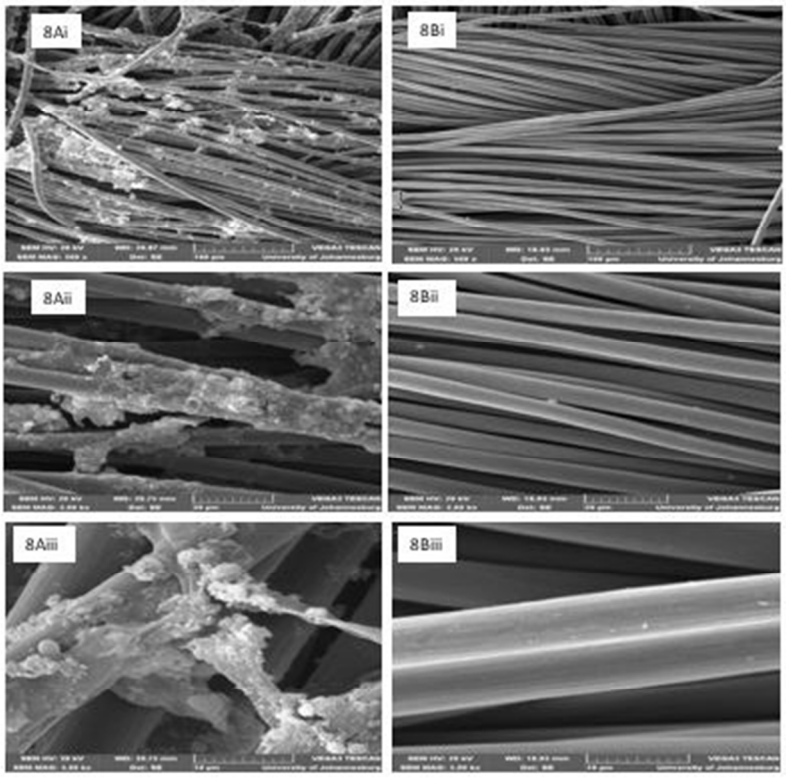

Scanning electron micrograph of anode (working electrode) inoculated with domestic wastewater (A) and (B) a control electrode (before inoculation)
109x121mm (96 x 96 DPI)

For Peer Review Only

Table 1 Mesh material and chemical composition

Material Type	Component element*	Specification (AISI 304) wt.%* Max	Min	Average specification* wt. %
AISI 304 Stainless steel. #20	C	0.08	–	0.051
	Mn	2.0	–	1.23
	Si	–	0.1	0.69
	P	0.045	–	0.021
	Ni	10.5	8.0	9.78
	Cr	20	18	18.91
	S	0.03	–	0.018

* Mesh information supplied by the manufacturer

Mesh material and chemical composition
95x118mm (96 x 96 DPI)

For Peer Review Only

Table 2 Selected maximum power densities using natural wastewater in MFCs

Substrate	MFC type	Maximum power density (mW/m^2)	Reference
Brewery wastewater	Air cathode single chamber	528	Feng et al., 2008
Corn Stover biomass	Air cathode single chamber bottle	406	Wang et al., 2009
Beer brewery wastewater	Air cathode single chamber	264	Wen et al., 2009
Swine wastewater	Air cathode single chamber	261	Min et al., 2005
Brewery wastewater	Air cathode single chamber	205	Feng et al., 2008
Domestic wastewater	Air cathode single chamber without PEM	146	Liu and Logan, 2004
Molasses wastewater	Anaerobic baffled stacking	115.5	Zhong et al., 2011
Full strength domestic wastewater	**Sandwich dual chamber**	**251**	**This work**
Swine wastewater	Dual chamber	45	Min et al., 2005
Urban wastewater	Dual chamber with salt bridge	25	Rodrigo et al., 2007

Selected maximum power densities using natural wastewater in MFCs
130x134mm (96 x 96 DPI)

Table 3 Summary of the wastewater treatment efficiency analysis of the MFC

Parameter (mg/L)	Percentage removed
COD	89
NO_3^-	77
NO_2^-	60
N	36
PO_4^{3-}	26

Summary of the wastewater treatment efficiency analysis of the MFC
140x94mm (96 x 96 DPI)

eview Only